USE OF B-SPLINE IN THE FINITE ELEMENT ANALYSIS: COMPARISON WITH ANCF GEOMETRY

Ahmed A. Shabana
Ashraf M. Hamed
Abdel - Nasser A. Mohamed

Department of Mechanical and Industrial Engineering
University of Illinois at Chicago
842 West Taylor Street
Chicago, Illinois 60607

Paramsothy Jayakumar
Michael D. Letherwood

U.S. Army RDECOM-TARDEC
6501 E. 11 Mile Road
Warren, MI 48397-5000

Report Documentation Page

Form Approved
OMB No. 0704-0188

1. REPORT DATE	2. REPORT TYPE	3. DATES COVERED
04 FEB 2011	**Journal Article**	**10-04-2010 to 24-10-2010**

4. TITLE AND SUBTITLE	5a. CONTRACT NUMBER
USE OF B-SPLINE IN THE FINITE ELEMENT ANALYSIS: COMPARISON WITH ANCF GEOMETRY	5b. GRANT NUMBER
	5c. PROGRAM ELEMENT NUMBER
6. AUTHOR(S)	5d. PROJECT NUMBER
Ahmed Shabana; Ashraf Hamed; Abdel - Nasser Mohamed; Paramsothy Jayakumar; Michael Letherwood	5e. TASK NUMBER
	5f. WORK UNIT NUMBER
7. PERFORMING ORGANIZATION NAME(S) AND ADDRESS(ES)	8. PERFORMING ORGANIZATION REPORT NUMBER
Department of Mechanical and Industrial Engineering,University of Illinois at Chicago,842 West Taylor Street,Chicago,Il,60607	**; #21484**
9. SPONSORING/MONITORING AGENCY NAME(S) AND ADDRESS(ES)	10. SPONSOR/MONITOR'S ACRONYM(S)
U.S. Army TARDEC, 6501 East Eleven Mile Rd, Warren, Mi, 48397-5000	**TARDEC**
	11. SPONSOR/MONITOR'S REPORT NUMBER(S)
	#21484

12. DISTRIBUTION/AVAILABILITY STATEMENT

Approved for public release; distribution unlimited

13. SUPPLEMENTARY NOTES

ASME 2011 IDETC: 8th International Conference on Multibody Systems, Nonlinear Dynamics, and Control

14. ABSTRACT

This paper examines the limitations of using B-spline representation as an analysis tool by comparing its geometry with the nonlinear finite element absolute nodal coordinate formulation (ANCF) geometry. It is shown that while both B-spline and ANCF geometries can be used to model non-structural discontinuities using linear connectivity conditions, there are fundamental differences between B-spline and ANCF geometries. First, while B-spline geometry can always be converted to ANCF geometry, the converse is not true; that is, ANCF geometry cannot always be converted to B-spline geometry. Second, because of the rigid structure of the B-spline recurrence formula, there are restrictions on the order of the parameters and basis functions used in the polynomial interpolation; this in turn can lead to models that have significantly larger number of degrees of freedom as compared to those obtained using ANCF geometry. Third, in addition to the known fact that B-spline does not allow for straight forward modeling of Tjunctions, B-spline representation cannot be used in a straight forward manner to model structural discontinuities. It is shown in this investigation that ANCF geometric description can be used to develop new spatial chain models governed by linear connectivity conditions which can be applied at a preprocessing stage allowing for an efficient elimination of the dependent variables. The modes of the deformations at the definition points of the joints that allow for rigid body rotations between ANCF finite elements are discussed. The use of the linear connectivity conditions with ANCF spatial finite elements leads to a constant inertia matrix and zero Coriolis and centrifugal forces. The fully parameterized structural ANCF finite elements used in this study allow for the deformation of the cross section and capture the coupling between this deformation and the stretch and bending. A new chain model that employs different degrees of continuity for different coordinates at the joint definition points is developed in this investigation. In the case of cubic polynomial approximation, 1 C continuity conditions are used for the coordinate line along the joint axis; while 0 C continuity conditions are used for the other coordinate lines. This allows for having arbitrary large rigid body rotation about the axis of the joint that connects two flexible links. Numerical examples are presented in order to demonstrate the use of the formulations developed in this paper.

15. SUBJECT TERMS

Geometric discontinuities; Finite element; Multibody systems; B-spline; NURBS

16. SECURITY CLASSIFICATION OF:			17. LIMITATION OF ABSTRACT	18. NUMBER OF PAGES	19a. NAME OF RESPONSIBLE PERSON
a. REPORT	b. ABSTRACT	c. THIS PAGE			
unclassified	**unclassified**	**unclassified**	**Public Release**	**33**	

ABSTRACT

This paper examines the limitations of using B-spline representation as an analysis tool by comparing its geometry with the nonlinear finite element *absolute nodal coordinate formulation* (ANCF) geometry. It is shown that while both B-spline and ANCF geometries can be used to model *non-structural discontinuities* using linear connectivity conditions, there are fundamental differences between B-spline and ANCF geometries. First, while B-spline geometry can always be converted to ANCF geometry, the converse is not true; that is, ANCF geometry cannot always be converted to B-spline geometry. Second, because of the rigid structure of the B-spline recurrence formula, there are restrictions on the order of the parameters and basis functions used in the polynomial interpolation; this in turn can lead to models that have significantly larger number of degrees of freedom as compared to those obtained using ANCF geometry. Third, in addition to the known fact that B-spline does not allow for straight forward modeling of T-junctions, B-spline representation cannot be used in a straight forward manner to model *structural discontinuities*. It is shown in this investigation that ANCF geometric description can be used to develop new spatial chain models governed by linear connectivity conditions which can be applied at a preprocessing stage allowing for an efficient elimination of the dependent variables. The modes of the deformations at the definition points of the joints that allow for rigid body rotations between ANCF finite elements are discussed. The use of the linear connectivity conditions with ANCF spatial finite elements leads to a constant inertia matrix and zero Coriolis and centrifugal forces. The fully parameterized structural ANCF finite elements used in this study allow for the deformation of the cross section and capture the coupling between this deformation and the stretch and bending. A new chain model that employs different degrees of continuity for different coordinates at the joint definition points is developed in this investigation. In the case of cubic polynomial approximation, C^1 continuity conditions are used for the coordinate line along the joint axis; while C^0 continuity conditions are used for the other coordinate lines. This allows for having arbitrary large rigid body rotation about the axis of the joint that connects two flexible links. Numerical examples are presented in order to demonstrate the use of the formulations developed in this paper.

Keywords: Geometric discontinuities; Finite element; Multibody systems; B-spline; NURBS.

1. INTRODUCTION

The geometry description used in many of the existing finite element (FE) formulations cannot be exactly converted to the geometry developed by computational geometry methods such as B-spline and NURBS (**N**on-**U**niform **R**ational **B**-**S**plines) representations. This fact has motivated researchers in the mechanics community to adopt the methods of computational geometry as analysis tools instead of using conventional FE formulations. While the methods of computational geometry, such as B-spline, have several desirable analysis features; these methods have serious limitations when used as analysis tools. The B-spline recurrence formula and the rigid definition of the knot vector make B-spline less attractive as compared to the *absolute nodal coordinate formulation* (ANCF) geometry description. While B-spline geometry can always be converted exactly to ANCF geometry (Piegl and Tiller, 1997, Sanborn and Shabana, 2009; Lan and Shabana, 2010), the converse is not always true. ANCF geometry does not restrict the order of the parameters or the number of basis functions used in the interpolating polynomials (Dmitrochenko.and Pogorelov, 2003; Dufva et al., 2005; Garcia-Vallejo et al., 2008; Kerkkänen et al., 2006; Schwab and Meijaard, 2010; Tian et al., 2009, 2010; Yoo et al., 2004; Yakoub and Shabana, 2001; Shabana and Mikkola, 2003; Abbas et al., 2010). This advantage, as will be demonstrated in this paper, allows for developing finite elements with less number of degrees of freedom as compared to those developed using the B-spline geometry. Another fundamental difference between B-spline and ANCF geometric descriptions lies in modeling discontinuities. As previously explained by the authors using simple planar examples, there are two types of discontinuities when chain systems are considered (Hamed et al., 2011). The first is *structural discontinuity* which does not allow rigid body displacement between two elements connected at the joint definition point. This joint allows only for deformation degrees of freedom. The second type of discontinuity is called *non-structural discontinuity* which allows

for rigid body displacement at the joint definition point. Figure 1 shows a chain which has a structural discontinuity at point C and non-structural discontinuity at point O. At the junction at C, only deformation degrees of freedom are allowed, while at point O, relative rigid body rotation is permitted. Nonetheless, the degree of continuity at both points is C^0. B-spline can be used as an analysis tool to describe the non-structural C^0 discontinuity at point O, but because of its rigid recurrence structure and the definition of its knot vector and knot multiplicity, B-spline cannot be used in the motion analysis of structural C^0 continuity at point C since B-spline C^0 description leads to a rigid body mode; that is, the elimination of one control point by reducing the knot multiplicity by one is not sufficient for eliminating the modes of rigid body rotations between two B-spline segments. ANCF geometry, on the other hand, can be used in the analysis of both structural and non-structural discontinuities (Hamed et al., 2011).

One of the important multibody system (MBS) applications that can be used to shed light on the fundamental differences between B-spline and ANCF geometries are chain applications. Chains are highly nonlinear systems that are subjected to repeated impulsive forces during their functional use. Geometric nonlinearities are the result of the large relative displacements between the chain links. The repeated impulsive forces as the result of the chain link contact with the rollers and other system components introduce high frequencies to the nonlinear chain dynamic model. For these reasons, the nonlinear dynamic analysis of chain systems represents one of the most challenging computational problems. In fact the simplest rigid-link chains are highly nonlinear because of the large relative rotations between the chain links (Roberson and Schwertassek, 1988; Schiehlen, 1997). In the case of rigid-link chains, the geometric nonlinearities that result from these rotations lead to highly nonlinear chain inertia forces that include the quadratic velocity Coriolis and centrifugal forces. Furthermore, the contact between

the rigid-chain links and the sprockets and rollers that may exist in the system is often described using compliant force models; leading to high frequencies that require the use of very small time integration step in order to accurately capture the changes in the velocities, accelerations, and forces. For these reasons, efficient and accurate modeling of chain systems remains a challenging MBS computational problem even in the simpler case in which the chain links are assumed to be rigid.

Because of the geometric nonlinearities and the high frequencies, it is important to use an efficient solution algorithm if the flexibility of the chain links is considered. Flexible-link chains require the use of significantly larger number of degrees of freedom in order to capture the link deformation modes. Some of these deformation modes may also introduce high frequencies in addition to the high frequencies resulting from the contact between the chain links and rollers as well as other components in the system. It is also important in some applications to capture certain coupled deformation modes that cannot be captured using conventional structural finite elements such as beams and plates that are based on simplified kinematic assumptions. For example, in tracked vehicle applications, the chain links are subjected to significant tensile and compressive forces. The coupling between the deformation of the link cross section and other modes of deformation can be significant and must be taken into account in order to develop a more realistic model. It is, therefore, important to employ FE formulation that captures the effect of these coupled deformation modes and allows for an efficient MBS implementation. It was shown in the literature using planar examples that ANCF finite elements can be used to develop new FE meshes for chain applications (Garcia de Valljo et al, 2003; Hamed et al, 2011). In these FE meshes, the flexible-link pin joints are defined using linear connectivity conditions despite the large relative rotation allowed between the chain links. This leads to an efficient elimination

of the dependent variables at a preprocessing stage. Furthermore, the use of the linear connectivity conditions with ANCF finite elements leads to a constant chain inertia matrix and zero Coriolis and centrifugal forces. It is one of the main objectives of this investigation to demonstrate for the first time that a three-dimensional flexible-link chain model that is based on linear connectivity conditions and has a constant mass matrix and zero Coriolis and centrifugal forces can be developed using spatial fully parameterized ANCF finite elements.

This paper focuses on two fundamental issues that summarize its main contributions. First, the fundamental differences between B-spline and ANCF geometries are demonstrated. It is shown that while B-spline geometry can always be converted to ANCF geometry, the converse is not true because of the rigid B-spline recurrence structure. It is also shown that B-spline representation can be used only in the analysis of one type of C^0 continuity referred to in this paper as non-structural discontinuity; while such a B-spline representation cannot be used in the analysis of another type of C^0 continuity referred to as structural discontinuity. It is shown that ANCF finite elements which have degrees of freedom less than their B-spline counterparts can be developed since ANCF does not have specific requirements on the order of the parameterization variables or the number of basis functions used in the interpolating polynomials.

The second main contribution of this paper is to develop a new three-dimensional flexible-link chain model using fully parameterized ANCF finite elements. This chain model is based on a new FE mesh defined using linear connectivity conditions. The FE mesh allows for relative rigid body rotations between its elements and has a constant inertia matrix and zero Coriolis and centrifugal forces. In order to develop the new flexible-link chain model presented in this paper, a new pin joint model is introduced. At the joint definition point, different degrees

of continuity are used with different parameters; leading to some strain components to be continuous while the others are discontinuous. The modes of deformation at the joint definition points are discussed in order to shed light on the nature of the new joint and kinematic constraints developed in this paper. Numerical results are presented in order to demonstrate the use of ANCF finite elements in developing the new flexible-link chain model. The limitations identified in this paper when B-spline geometry is used as analysis tool suggest the use of the *integration of computer aided design and analysis* (I-CAD-A) approach (Sanborn and Shabana, 2009; Lan and Shabana, 2010). In the I-CAD-A approach, a constant transformation can be developed to convert CAD geometry to FE mesh.

2. B-SPLINE SURFACES

B-spline surfaces are defined using the product of B-spline base functions, two parameters, and two knot vectors. B-spline surfaces can be defined in the following parametric form (Piegl and Tiller, 1997):

$$\mathbf{r}(u,v)=\sum_{i=0}^{n}\sum_{j=0}^{m}N_{i,p}(u)N_{j,q}(v)\mathbf{P}_{i,j} \tag{1}$$

where u and v are the parameters; $N_{i,p}(u)$ and $N_{j,q}(v)$ are B-spline basis functions of degree p and q, respectively; and $\mathbf{P}_{i,j}$ are a set of bidirectional net of control points. The B-spline basis functions $N_{i,p}(u)$ are defined as

$$\left.\begin{aligned} N_{i,0}(u) &= \begin{cases} 1 & \text{if } u_i \le u < u_{i+1} \\ 0 & \text{otherwise} \end{cases} \\ N_{i,j}(u) &= \frac{u-u_i}{u_{i+j}-u_i} N_{i,j-1}(u) + \frac{u_{i+j+1}-u}{u_{i+j+1}-u_{i+1}} N_{i+1,j-1}(u) \end{aligned}\right\} \qquad (2)$$

where u_i, $i = 0,1,2,\ldots,n+p+1$ are called the *knots*; and $u_i \le u_{i+1}$. The vector $\mathbf{U} = \{u_0 \quad u_1 \quad \cdots \quad u_{n+p+1}\}$ is called the *knot vector*. Similar definitions can be introduced for $N_{j,q}(v)$ with another knot vector $\mathbf{V} = \{v_0 \quad v_1 \quad \cdots \quad v_{m+q+1}\}$. Note that the orders of the polynomials in the u and v directions can be different; for example, a cubic interpolation can be used along u while a linear interpolation can be used along v. As in the case of B-spline curves, the knots of B-spline surfaces do not have to be distinct; distinct knots are called *breakpoints* and define surface segments with non-zero dimensions. The number of the non-distinct knots in $\mathbf{U}$ and $\mathbf{V}$ at a point is referred to as the knot multiplicity associated, respectively, with the parameters u and v at this point. At a given breakpoint, the multiplicity associated with u can be different from the multiplicity associated with v; allowing for different degrees of continuity for the derivatives with respect to u and v. For cubic $N_{i,p}$ ($p = 3$), C^0, C^1, or C^2 conditions correspond, respectively, to knot multiplicity of three, two, and one; while in the case of linear interpolation of $N_{j,q}$, the highest continuity degree that can be demanded is continuity of the gradients. When zero multiplicity is used at a breakpoint, the segments blend together at this point.

In B-spline surface representation, there is a relationship between the polynomial degree, the number of knots, and the number of control points. This relationship must be fully understood if B-spline geometry will be used as an analysis tool. If $r+1$ is the number of knots in $\mathbf{U}$ and $s+1$ is the number of knots in $\mathbf{V}$, then in B-spline geometry, one must have

$$r = n + p + 1, \quad s = m + q + 1 \tag{3}$$

These formulas imply that, for a given polynomial order, if the number of knots decreases, the number of control points (degrees of freedom used in the analysis) must also decrease. A decrease in the knot multiplicity by one is equivalent to eliminating one control point. This can also be equivalent to increasing the degree of continuity since eliminating a control point can be the result of imposing algebraic equations that relates the derivatives at a certain breakpoint. From the bidirectional structure used in Eq. 1, a surface segment which has cubic interpolation along u ($p = 3, n = 3, r + 1 = 8$) and a linear interpolation along v ($q = 1, m = 1, s + 1 = 4$), should have $(n+1)\times(m+1) = 8$ control points; this is regardless of whether the surface is two- or three-dimensional. Manipulation of the B-spline surface of Eq. 1 shows that these eight control points are the result of using the alternate basis set $1, u, v, uv, u^2, u^2v, u^3, u^3v$. That is, B-spline representation and the formulas of Eq. 3 do not allow for the use of the basis set $1, u, v, uv, u^2, u^3$ which can be effectively used to develop a shear deformable beam model. If a cubic interpolation is used for both u and v (thin plate), the B-spline representation will require 16 control points because the expansion must include all terms $u^k v^l$; $k, l = 0, 1, 2, 3$ regardless of whether the shape of deformation of the plate is simple or complex; one must strictly follow the B-spline rigid structure. This can be of disadvantage in the analysis since such a geometric representation can unnecessarily increase the dimension of the analysis model and leads to the loss of the flexibility offered by the FE method or modal analysis techniques. As the degree of the polynomial interpolation increases, the problem gets even worse. Another important and interesting issue with regard to the use of B-spline as an analysis tool is capturing discontinuities; this is discussed in the following section.

3. STRUCTURAL AND NON-STRUCTURAL DISCONTINUITIES

As previously mentioned, in the case of structural discontinuity, there is no relative rigid body motion at the discontinuity node; all the relative displacements are due to deformations. Example of structural discontinuity is at point C in Fig.1. At the structural discontinuity node, in the case of the planar system shown in Fig. 1, there is only one state of strains. Non-structural discontinuity, on the other hand, allows for relative rigid body rotation. At point O of Fig. 1, there can be two different states of strains because of the rigid body mode. Nonetheless, structural and non-structural discontinuities can be classified as C^0. They are, however, fundamentally different from the analysis point of view since they lead to completely two different joint models that have different numbers of degrees of freedom. Interestingly, one of these types of discontinuities can be captured by B-spline recurrence formula, while the other cannot be captured. More interestingly, the discontinuity type captured by B-spline is the non-structural discontinuity that characterizes many mechanical system applications. Modeling structural discontinuity that characterizes both mechanical and structural systems requires the use gradient transformation which is crucial in the ANCF geometric representation.

As previously mentioned, reducing the knot multiplicity by one at a breakpoint leads to C^0 continuity and to the elimination of one control point. This equivalent to the MBS pin joint constraint definition in planar analysis and to the MBS spherical joint definition in the spatial analysis. This type of C^0 continuity that is captured by B-spline is of the non-structural discontinuity type which leads to a rigid body mode and to a non-unique state of the strain at the discontinuity node. The B-spline recurrence formula structure leads automatically to this type of discontinuity. The structural discontinuity, while it is also of the C^0 type, requires additional algebraic equations in order to define a unique strain state by eliminating the relative rotation at

the joint definition point. These algebraic equations can be used to eliminate other control points, and such elimination is not embedded in the rigid B-spline geometry representation. Only one type of C^0 continuity that can be achieved by using B-spline formula; reducing the knot multiplicity by one in B-spline representation does not capture structural discontinuity.

4. GENERALITY OF ANCF GEOMETRY

While B-spline geometry can always be converted to ANCF geometry, the converse is not true. ANCF geometry does not impose restriction on the basis functions that must be included in the interpolating polynomials. This allows for developing finite elements that have less coordinates as compared to those developed using the B-spline representation. Furthermore, ANCF geometry can be used to model both structural and non-structural discontinuities (Shabana and Mikkola, 2003; Shabana, 2010; Hamed et al., 2011), while the rigid recurrence B-spline representation cannot be used to model structural discontinuities in a straight forward manner. The basic differences between ANCF and B-spline geometries are demonstrated in this section using a planar beam example. The displacement field of the shear deformable beam used in this section can be written as $\mathbf{r}(x,y)=\mathbf{S}(x,y)\mathbf{e}(t)$, where x and y are the element spatial coordinates, t is time, $\mathbf{S}$ is the element shape function matrix, and $\mathbf{e}$ is the vector of the element nodal coordinates. The shape function matrix for the element considered in this section is defined as

$$\mathbf{S}^j=\begin{bmatrix} s_1\mathbf{I} & s_2\mathbf{I} & s_3\mathbf{I} & s_4\mathbf{I} & s_5\mathbf{I} & s_6\mathbf{I}\end{bmatrix} \tag{4}$$

where the shape functions s_i, $i=1,2,\ldots,6$ are defined as (Omar and Shabana, 2001)

$$\left.\begin{aligned} s_1 &= 1-3\xi^2+2\xi^3, \quad s_2 = l\left(\xi-2\xi^2+\xi^3\right), \quad s_3 = l\eta\left(1-\xi\right), \\ s_4 &= 3\xi^2-2\xi^3, \quad s_5 = l\left(-\xi^2+\xi^3\right), \quad s_6 = l\xi\eta \end{aligned}\right\} \tag{5}$$

In this equation, $\xi = x/l$, $\eta = y/l$. ANCF finite elements employ gradient vectors as nodal coordinates. For the element used in this section, the vector of nodal coordinates is defined as

$$\mathbf{e} = \left[\left(\mathbf{r}\right)_1^T \quad \left(\partial\mathbf{r}/\partial x\right)_1^T \quad \left(\partial\mathbf{r}/\partial y\right)_1^T \quad \left(\mathbf{r}\right)_2^T \quad \left(\partial\mathbf{r}/\partial x\right)_2^T \quad \left(\partial\mathbf{r}/\partial y\right)_2^T\right]^T \tag{6}$$

where $\left(\ \right)_k$, $k = 1,2$ indicates variables evaluated at node k of the element. Note that the element defined by the preceding equations is based on a cubic interpolation for x and a linear interpolation for y. This element has been widely used in the analysis of large deformation problems.

The finite element described in this section is an example of ANCF elements that cannot be converted to B-spline representation. This element is based on a polynomial expansion that does not have the two basis functions x^2y and x^3y. These terms can be systematically included in ANCF geometry by adding nodal coordinates allowing for converting B-spline representation to ANCF representation. Similar comments apply to ANCF thin plate elements that do not have to include all the basis functions $x^k y^l; k,l = 0,1,2,3$. This flexibility offered by ANCF geometry allows for developing finite elements that have smaller number of coordinates compared to those elements developed by B-spline geometry.

One can also show that ANCF finite elements can describe structural and non-structural discontinuities. Non-structural discontinuities that allow for large rigid body rotations can be described using a C^0 model obtained by imposing constraints on the position coordinates only.

For example if two elements i and j are connected by pin joint at a node, one can apply the algebraic equations $\mathbf{r}^i = \mathbf{r}^j$ at this node. These algebraic equations can be imposed at a preprocessing stage to eliminate the dependent variables and define FE mesh that has a constant mass matrix and zero Coriolis and centrifugal forces despite the finite rotations allowed between the finite elements of the mesh. As previously mentioned, non-structural discontinuities can also be described using B-spline geometry by reducing the knot multiplicity at the joint node by one. Note that in the case of non-structural discontinuities no constraints are imposed on the gradient vectors, and therefore, the state of strain is not unique at the joint node. Each of the Lagrangian strains $\varepsilon_{xx} = \left(\mathbf{r}_x^T \mathbf{r}_x - 1\right)/2$, $\varepsilon_{yy} = \left(\mathbf{r}_y^T \mathbf{r}_y - 1\right)/2$, and $\varepsilon_{xy} = \mathbf{r}_x^T \mathbf{r}_y /2$ have two values at the joint node; one defined on element i and the other is defined on element j. Here $\mathbf{r}_x = \partial \mathbf{r}/\partial x$, $\mathbf{r}_y = \partial \mathbf{r}/\partial y$, $\mathbf{r}_z = \partial \mathbf{r}/\partial z$.

The concept of degrees of freedom widely used in mechanics is not considered in developing the recurrence relationships on which B-spline and NURBS geometry are based. This represents another serious limitation when these computational geometry methods are used as analysis tools; as evident by the fact that B-spline geometry cannot describe structural discontinuities. This type of discontinuities, while it remains of the C^0 continuity type, requires imposing additional constraints on the gradients; these constraints cannot be captured by the B-spline recurrence formula since they require the elimination of additional vectors. In the case of B-spline, C^0 continuity is achieved by reducing the knot multiplicity by one, and this eliminates one control point leading to the definition of a pin joint (non-structural discontinuity). ANCF geometry, on the other hand, allows for imposing constraints on the gradients using the tensor transformation $\left(\partial \mathbf{r}/\partial \mathbf{x}_1\right) = \left(\partial \mathbf{r}/\partial \mathbf{x}_2\right)\mathbf{A}$, where $\mathbf{x}_1 = \begin{bmatrix} x_1 & y_1 \end{bmatrix}^T$ and $\mathbf{x}_2 = \begin{bmatrix} x_2 & y_2 \end{bmatrix}^T$ are two sets of

coordinate lines, and $\mathbf{A}$ is the matrix of coordinate line transformation. Using this tensor gradient transformation, the structural discontinuities can be systematically modeled using ANCF finite elements (Shabana and Mikkola, 2003; Shabana, 2010). For example, if the axis of a beam element j makes an angle α with the axis of another element i and the two elements are rigidly connected at a node, the structural discontinuity conditions that eliminate all the relative rigid body displacements can be written at the joint node as

$$\mathbf{r}^i = \mathbf{r}^j, \qquad \begin{bmatrix} \dfrac{\partial \mathbf{r}^i}{\partial x^i} & \dfrac{\partial \mathbf{r}^i}{\partial y^i} \end{bmatrix} = \begin{bmatrix} \dfrac{\partial \mathbf{r}^j}{\partial x^j} & \dfrac{\partial \mathbf{r}^j}{\partial y^j} \end{bmatrix} \begin{bmatrix} \cos\alpha & \sin\alpha \\ -\sin\alpha & \cos\alpha \end{bmatrix} \tag{7}$$

These six scalar algebraic equations can be used to eliminate a position coordinate vector and two gradient vectors, defining a unique strain state at the node of connectivity between the ANCF finite elements. The algebraic conditions of Eq. 7 that allow ANCF finite elements to describe two types of C^0 discontinuity cannot be automatically captured by the B-spline recurrence formula. Note that these algebraic conditions are linear in the ANCF finite element coordinates, and therefore, they can be applied using a standard FE assembly procedure at a preprocessing stage of the analysis. These conditions lead to a relative motion, between the finite elements, that is pure deformation displacement.

It is important to point out that the coordinate line transformation of Eq. 7 need to be applied only in the case of structural discontinuities. Such a transformation is not required in the case of non-structural discontinuities despite the fact that the elements can have arbitrary orientation relative to each others. This is due to facts that non-structural discontinuity does not impose constraints on the gradient vectors, ANCF geometry is invariant under an arbitrary rigid body displacement, and each ANCF finite element has its own independent parameters.

Similarly, in the case of curved shapes as in belt applications, the coordinate transformation used in Eq.7 is not required since there are no structural discontinuities and the gradients at all points on the belt can be defined with respect to the same coordinate lines. In the curved sections of the belt, one must provide the appropriate values of the gradient vectors that define the correct shape. Recall that a curve, regardless of its shape, requires only one parameter; while a surface, regardless of its shape, requires only two parameters.

5. THREE-DIMENSIONAL NON-STRUCTURAL DISCONTINUITIES

In this section, it is shown how fully parameterized ANCF three-dimensional finite elements can be used to develop spatial joint models that allow large relative rigid body rotation between the finite elements. ANCF finite elements connected by this joint can be assembled using linear connectivity conditions leading to FE mesh that has a constant mass matrix and zero Coriolis and centrifugal forces. The fully parameterized three-dimensional ANCF beam element is used in this investigation to demonstrate the development of such joint models. The displacement field of the element can be written as $\mathbf{r}(x,y,z)=\mathbf{S}(x,y,z)\mathbf{e}(t)$ where x, y, and z are the element spatial coordinates. The shape function matrix of this element is defined as (Yakoub and Shabana, 2001; Shabana, 2008)

$$\mathbf{S}=\begin{bmatrix} s_1\mathbf{I} & s_2\mathbf{I} & s_3\mathbf{I} & s_4\mathbf{I} & s_5\mathbf{I} & s_6\mathbf{I} & s_7\mathbf{I} & s_8\mathbf{I} \end{bmatrix} \tag{8}$$

where the shape functions s_i, $i=1,2,\ldots,8$ are defined as

$$\left.\begin{aligned} &s_1=1-3\xi^2+2\xi^3, \quad s_2=l\left(\xi-2\xi^2+\xi^3\right),\\ &s_3=l\left(\eta-\xi\eta\right), \quad s_4=l\left(\varsigma-\xi\varsigma\right), \quad s_5=3\xi^2-2\xi^3,\\ &s_6=l\left(-\xi^2+\xi^3\right), \quad s_7=l\xi\eta, \quad s_8=l\xi\varsigma \end{aligned}\right\} \tag{9}$$

In this equation, $\xi = x/l, \eta = y/l, \varsigma = z/l$. The element has two nodes; each node has 12 nodal coordinates defined by the vector $\mathbf{e}^k = \begin{bmatrix} \mathbf{r}^{kT} & \mathbf{r}_x^{kT} & \mathbf{r}_y^{kT} & \mathbf{r}_z^{kT} \end{bmatrix}^T$, where k is the node number. The ANCF finite element defined by Eqs. 8 and 9 captures the cross section deformation and its coupling with extension and bending. Therefore, this element can be used to develop general models for belt drives and rubber tracked vehicles.

The three-dimensional beam element presented in this section is another example that can be used to demonstrate the generality of the ANCF geometry. This element is based on cubic interpolation in x and linear interpolation in y and z. Nonetheless, one can show that the four basis functions x^2y, x^3y, x^2z, x^3z are not used in developing the displacement field of this widely used ANCF beam element. Therefore, the geometry of this element cannot be converted to B-spline volume geometry. These missing basis functions can be systematically included in the development of another ANCF finite element that can be converted to B-spline volume geometry. However, such an element will lead to 50% increase in the number of the element nodal coordinates.

A planar pin joint between rigid or flexible bodies is an example of C^0 continuity, as previously discussed. A pin joint between two rigid bodies in the spatial analysis also allows for only one degree of freedom, which is a relative rotation about the joint axis. Since the pin joint eliminates five degrees of freedom in the rigid body analysis, its formulation requires five algebraic constraint equations that eliminate three relative translation displacements and two relative rotations between the two bodies. In the case of flexible bodies, an infinitesimal volume can have 12 modes of displacements; three rigid body translations, three rotations, and six deformation modes. In this section, a new model of pin joint between ANCF finite elements is

introduced. The formulation of this pin joint between elements i and j employs the following six scalar equations defined at the joint node:

$$\mathbf{r}^i = \mathbf{r}^j, \qquad \mathbf{r}_\alpha^i = \mathbf{r}_\alpha^j \tag{10}$$

Here α is the coordinate line that defines the joint axis; α can be x, y, or z or any other coordinate line as discussed later in this section. The six scalar equations of Eq. 10 eliminate six degrees of freedom; three translations, two rotations, and one deformation mode. This joint model ensures C^1 continuity with respect to the coordinate line α and C^0 continuity with respect to the other two parameters. It follows that the Lagrangian strain component $\varepsilon_{\alpha\alpha} = \left(\mathbf{r}_\alpha^T \mathbf{r}_\alpha - 1\right)/2$ is continuous at the joint definition point, while the other five strain components can be discontinuous.

While the algebraic constraint equations of a pin joint between two rigid bodies are highly nonlinear. The algebraic constraint equations of Eq. 10 are linear. Therefore, these equations can be applied at a preprocessing stage to systematically eliminate the dependent variables. Using these equations, one can develop a new kinematically linear FE mesh for flexible-link chains in which the links can have arbitrarily large relative rotations. The use of this pin joint model with ANCF finite elements leads to a constant mass matrix and zero Coriolis and centrifugal forces.

As previously mentioned in this paper, B-spline geometry can describe the type of non-structural discontinuity discussed in this section. Nonetheless, if an arbitrary axis of a pin joint is to be used in the analysis, the use of B-spline geometry can be difficult given the rigid structure of the B-spline recurrence formula. In order to be able to choose an arbitrary axis of rotation for

the pin joint, one must be able to define the gradient vector in the direction of a coordinate line along this axis of rotation. Such a definition can be easily made using ANCF geometry using the gradient tensor transformation. Let u, v, and w be another set of parameters; one of them can be used to define the joint axis. It follows that $\begin{bmatrix}\mathbf{r}_u & \mathbf{r}_v & \mathbf{r}_w\end{bmatrix} = \begin{bmatrix}\mathbf{r}_x & \mathbf{r}_y & \mathbf{r}_z\end{bmatrix}\mathbf{A}$, where $\mathbf{A}$ is the constant matrix of coordinate transformation defined as

$$\mathbf{A} = \begin{bmatrix} \frac{\partial x}{\partial u} & \frac{\partial x}{\partial v} & \frac{\partial x}{\partial w} \\ \frac{\partial y}{\partial u} & \frac{\partial y}{\partial v} & \frac{\partial y}{\partial w} \\ \frac{\partial z}{\partial u} & \frac{\partial z}{\partial v} & \frac{\partial z}{\partial w} \end{bmatrix} \tag{11}$$

The fact that this matrix is constant allows having linear pin joint connectivity conditions when ANCF finite elements are used (Shabana and Mikkola, 2003; Shabana, 2010).

6. NUMERICAL EXAMPLES

In this section, three-dimensional belt drive and chain examples are used to demonstrate the implementation of the concepts discussed in this paper. The degree of continuity at the element interfaces can be applied at a preprocessing stage in order to eliminate the dependent variables leading to a finite element mesh that has a constant mass matrix and zero Coriolis and centrifugal forces. The fully parameterized three-dimensional ANCF beam element discussed in this paper is used in modeling the belt and the chain used in this section. The following three different models are considered in this section:

1. A finite element belt model with C^1 continuity. The geometry of this model can be defined in the initial configuration using a smooth curve that defines the centerline of the

belt. This model, referred to in this section as the C^1 belt model, leads to continuous gradients and strains at the element interfaces.

2. A finite element belt model that ensures continuity of $\mathbf{r}_y$ (C^1 continuity along y), but it has C^0 continuity along x and z. In the initial configuration, the centerline of the belt is continuous. This model is referred to as the C^0/C^1 belt model.

3. A finite element flexible-link chain model that ensures continuity of $\mathbf{r}_y$ (C^1 continuity along y), but it has C^0 continuity along x and z. This model differs from the previous two models due to the fact that the chain centerline is not continuous at the initial configuration because $\mathbf{r}_x$ and $\mathbf{r}_z$ are not continuous. This model will be referred to in this section as the chain model.

The belt and chain drive mechanisms considered in this section are assumed to consist of two pulleys and a flexible belt or a chain as shown in Figs. 2 and 3. Figure 3 shows the discontinuity of the gradients at the joints in the initial configuration. The pulleys are connected to the ground using revolute joints. The span length in the reference configuration is assumed to be 0.12 m in the case of the belt model and 0.128 m in the case of the chain model. In the examples considered in this section, the angular velocity of the driving pulley is specified by the following equation:

$$\omega_1 = \begin{cases} 0 & t \le 0.3 \\ 100\dfrac{(t-0.3)}{0.7} & 0.3 < t \le 1.0 \\ 100 & t > 1.0 \end{cases} \tag{12}$$

where ω_1 is expressed in rad/s, and t is the time expressed in seconds. The mass moment of inertia of the driven pulley about its axis of rotation is 0.0075 kg/m^2. In order to introduce

tension in the system, the driving pulley is displaced in the X direction until the span length reaches 0.18 m for the three models. In order to avoid oscillations at the beginning of the simulation, this pulley displacement is achieved over a period of 0.2 s. A resistance moment defined by the following equation is also applied to the driven pulley:

$$M = \begin{cases} 0 & t \le 0.3 \\ -1.1\dfrac{(t-0.3)}{0.7} & 0.3 < t \le 1.0 \\ -1.1 & t > 1.0 \end{cases} \tag{13}$$

The two pulleys are assumed to have the same radius and width of 0.058 and 0.01 m, respectively. A compliant force model is used to describe the belt/pulley interaction. The stiffness and damping coefficients used in the belt/pulley contact force model are given respectively by 9×10^7 N/m^3 and 2×10^3 N.s/m^3. Tangential friction forces are also introduced using a coefficient of dry friction of 1.2 (Leamy and Wasfy, 2002). The friction parameter that defines the slope in the transition region is assumed to be 10^6 N.s/m^3 (Dufva et al, 2007). The belt is modeled using 20 ANCF three-dimensional beam elements. Incompressible Neo-Hookean constitutive model with nonlinear damping model is used to model the flexible belt. The belt is assumed to have a rectangular cross-section of dimensions 0.01×0.004 m and density of 3500 kg/m^3. The incompressible Neo-Hookean model constant is assumed to be $\mu_s = 2\times10^6$ N/m^2, the incompressibility constant is assumed to be $k = 10^8$ N/m^2, and the dilatation and deviatoric dissipation factors used for the damping model are assumed to be 10^{-4} and 5×10^{-5}, respectively.

Figure 4 shows the angular velocity of the driving and driven pulleys for both the C^1, C^0/C^1, and chain models. The results presented in this figure show that the angular velocity of

the driven pulley in the case of the C^1 belt model is higher than that of C^0/C^1 belt and chain models. This can be attributed to the fact that in the case of the C^0/C^1 and chain models, some of the loads such as bending moment about Y axis are not transferred between elements. Figures 5-7 show the configurations of the belt centerline for the three models at time 1 s. These figures show that the gradients $\mathbf{r}_x$ and $\mathbf{r}_z$ are discontinuous in case of the C^0/C^1 belt and chain models and they are continuous in case of the C^1 belt model.

Figure 8 shows a measure of the cross section deformation along the belt centerline at time 1.9s. This measure is defined by Nanson's formula that can be used to calculate the ratio between the areas in the current and reference configurations. Nanson's formula is defined as (Ogden, 1984; Shabana, 2008)

$$\frac{da}{dA} = \frac{J}{\left(\mathbf{n}_n^T \mathbf{J}\mathbf{J}^T \mathbf{n}_n\right)} \tag{14}$$

where a and A are, respectively. The area in the current and the reference configurations, J is the determinant of the matrix of position vector gradients $\mathbf{J}$, and $\mathbf{n}_n$ is the unit vector normal to the area. The results of Fig. 8 show that the area ratio is continuous in the case of the C^1 belt model while it is not continuous in case of the C^0/C^1 and chain models. Figures 9-11 show comparison of the normal strains at the element interface points along the belt centerline for the three models. The results obtained in this investigation show that all the strain components, which are functions of the gradient vectors, are continuous in the case of the C^1 belt model; while in the case of the C^0/C^1 and chain models only ε_{yy} is continuous. Figure 12 shows the Lagrangian shear strain component ε_{xz} along the belt centerline. The results of this figure show

ε_{xz} to be discontinuous in the case of the C^0/C^1 and chain models because it is function of both the gradient vectors $\mathbf{r}_x$ and $\mathbf{r}_z$, which are discontinuous when these models are used.

7. SUMMARY AND CONCLUSIONS

This paper addresses the important issue of using computational geometry methods such as B-spline and NURBS as analysis tools. B-spline and NURBS employ recurrence formulas that allow changing the degree of continuity at a breakpoint by adjusting the knot multiplicity at this point. As demonstrated in this paper, the recurrence formula has several drawbacks when B-spline representation is used as an analysis tool. Because the recurrence formula does not provide flexibility for choosing the basis functions, B-spline representation can lead to significantly larger number of coordinates and a higher dimensional model. This fact was used to demonstrate the generality of the ANCF geometry. While B-spline geometry can always be converted to ANCF geometry, the converse is not true. It is also shown that the B-spline recurrence formula cannot be used to model structural discontinuity in a straight forward manner. While structural discontinuities are of the C^0 type, they cannot be captured in the B-spline representation by reducing the knot multiplicity by one. This reduction of the knot multiplicity is equivalent to elimination of the relative translation only; and such a reduction in the knot multiplicity leads to a rigid body mode that defines the conditions of a pin joint. In the case of structural discontinuities, on the other hand, the C^0 B-spline representation does not eliminate the rigid body mode since additional algebraic constraint equations are required in order to eliminate the relative rotations between two segments. The paper also presents a new three-dimensional pin joint model that leads to linear connectivity conditions and constant mass matrix when used with ANCF finite elements. The implementation of this new model is demonstrated using a flexible-

link chain example. The limitations identified in this paper when B-spline geometry is used as analysis tool suggest the use of the I-CAD-A approach in which a constant transformation can be developed to convert CAD geometry to FE mesh. It should be also clear that NURBS geometry has the same limitations as B-spline representation when used as an analysis tool.

ACKNOWLEDGEMENTS

This research was supported by the U.S. Army Research Office, Research Triangle Park, North Carolina; and, in part, by the National Science Foundation Office of International Programs (Project # 0808399).

REFRENCES

1. Abbas, L.K., Rui, X., and Hammoudi, Z.S., 2010, "Plate/Shell Element of Variable Thickness Based on the Absolute Nodal Coordinate Formulation", *IMechE Journal of Multibody Dynamics*, Vol. 224, Part K, pp. 127-141.
2. Dmitrochenko, O. N. and Pogorelov, D. Y., 2003, "Generalization of Plate Finite Elements for Absolute Nodal Coordinate Formulation", *Multibody System Dynamics*, Vol. 10, no. 1: 17-43.
3. Dufva, K., Kerkkanen, K., Maqueda, L.G., and Shabana, A.A., 2007, "Nonlinear Dynamics of Three-Dimensional Belt Drives Using the Finite Element Method", *Nonlinear Dynamics*, Vol. 48, pp. 449-466.
4. Dufva, K.E., Sopanen, J.T., and Mikkola, A.M., 2005, "A Two-Dimensional Shear Deformable Beam Element Based on the Absolute Nodal Coordinate Formulation", *Sound and Vibration*, Vol. 280, pp. 719-738.
5. Garcia-Vallejo, D., Escalona, J.L., Mayo, J., and Dominguez, J., 2003, "Describing Rigid-Flexible Multibody Systems Using Absolute Coordinates", *Nonlinear Dynamics*, Vol. 34, pp. 75-94.
6. Garcia-Vallejo, D., Mayo, J., and Escalona, J. L., 2008, "Three-Dimensional Formulation of Rigid-Flexible Multibody Systems with Flexible Beam Elements", *Multibody System Dynamics*, Vol. 20 (1), pp. 1-28.
7. Hamed, A.M., Shabana, A.A., Jayakumar, P., and Letherwood, M.D., 2011 "Non-Structural Geometric Discontinuities in Finite Element/Multibody System Analysis", *Nonlinear Dynamics*, in press.

8. Kerkkänen, K.S., García-Vallejo, D., and Mikkola, A.M., 2006, "Modeling of Belt-Drives using a Large Deformation Finite Element Formulation", *Nonlinear Dynamics*, Vol.43, pp. 239-256.
9. Lan, P., and Shabana, A.A., 2010, "Integration of B-spline Geometry and ANCF Finite Element Analysis". *Nonlinear Dynamics*, DOI 10.1007/s11071-009-9641-6.
10. Leamy, M.J., and Wasfy, T.M., 2002, "Analysis of belt-drive mechanics using a creep-rate-dependent friction law", *ASME Journal of Applied Mechanics*, Vol. 69, pp. 763-771.
11. Ogden, R.W., 1984, *Non-Linear Elastic Deformations*, Dover, New York.
12. Omar, M.A., Shabana, A.A.2001 "A Two-Dimensional Shear Deformation Beam for Large Rotation and Deformation", *Journal of Sound and Vibration*, Vol. 243(3), pp. 565–576.
13. Piegl, L. and Tiller, 1997, W.: "*The NURBS Book*", 2nd edn. Springer, New York.
14. Roberson, R.E., and Schwertassek, R., 1988, *Dynamics of Multibody Systems*, Springer Verlag, Berlin, Germany.
15. Sanborn, G.G. and Shabana, A.A., 2009, "On The Integration of Computer Aided Design and Analysis Using The Finite Element Absolute Nodal Coordinate Formulation", *Multibody System Dynamics*, Vol. 22, pp. 181–197.
16. Schiehlen, W.O., 1997, "Multibody System Dynamics: Roots and Perspectives", *Multibody System Dynamics*, Vol. 1, pp.149-188.
17. Schwab, A. L., and Meijaard, J. P., 2010, "Comparison of Three-Dimensional Flexible Beam Elements for Dynamic Analysis: Classical Finite Element Formulation and Absolute Nodal Coordinate Formulation", *Journal of Computational and Nonlinear Dynamics*, Vol. 5 (1), 011010-1 – 011010-10.

18. Shabana, A.A., 2008, "*Computational Continuum Mechanics*". Cambridge University Press, Cambridge.
19. Shabana, A.A., 2010,"General Method for Modeling Slope Discontinuities and T-Sections using ANCF Gradient Deficient Finite Elements", *ASME Journal of Computational and Nonlinear Dynamics*, (in press).
20. Shabana, A.A., and Mikkola, A.M., 2003, "Use of the Finite Element Absolute Nodal Coordinate Formulation in Modeling Slope Discontinuity", *ASME Journal for* Mechanical *Design*, Vol. 125(2), pp. 342–350.
21. Tian, Q., Chen, L.P., Zhang, Y.Q., Yang, J.Z., 2009 "An Efficient Hybrid Method for Multibody Dynamics Simulation Based on Absolute Nodal Coordinate Formulation", *ASME Journal of Computational and Nonlinear Dynamics*, Vol. 4, pp. 021009-1 - 021009-14.
22. Tian, Q., Zhang, Y., Chen, L., and Yang, J., 2010, "Simulation of Planar Flexible Multibody Systems with Clearance and Lubricated Revolute Joints", *Nonlinear Dynamics*, Vol. 60, pp. 489-511.
23. Yakoub, R.Y., and Shabana, A. A., 2001, "Three Dimensional Absolute Nodal Coordinate Formulation for Beam Elements: Implementation and Application", *ASME Journal for Mechanical Design*, Vol. 123, pp. 614–621.
24. Yoo, W.S., Lee, J.H., Park, S.J., Sohn, J.H.. Pogorelov, D., and Dimitrochenko, O., 2004, "Large Deflection Analysis of a Thin Plate: Computer Simulation and Experiment", *Multibody System Dynamics*, Vol. 11, pp. 185-208.

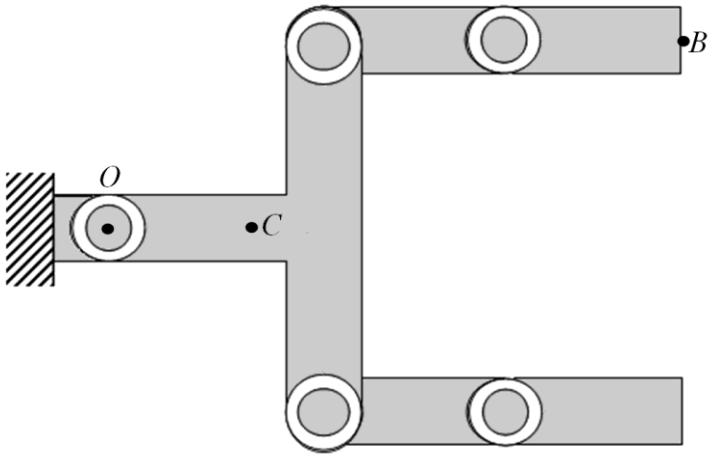

Figure 1 Structural and non-structural discontinuities

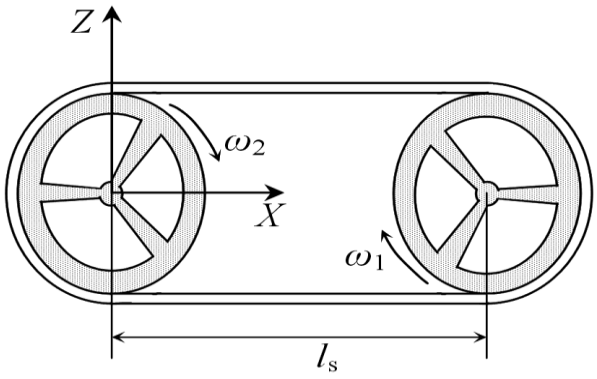

Figure 2 Initial configuration of the belt drive mechanism for both C^0/C^1 and C^1 models

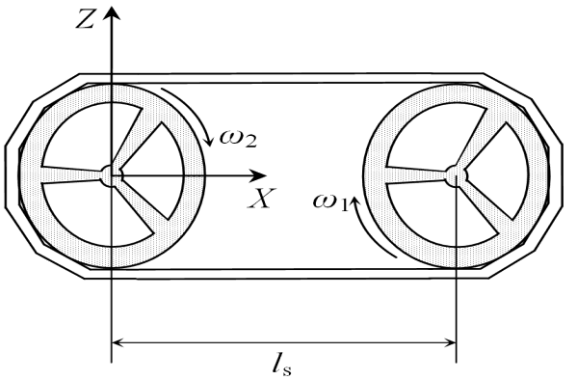

Figure 3 Initial configuration of the chain model

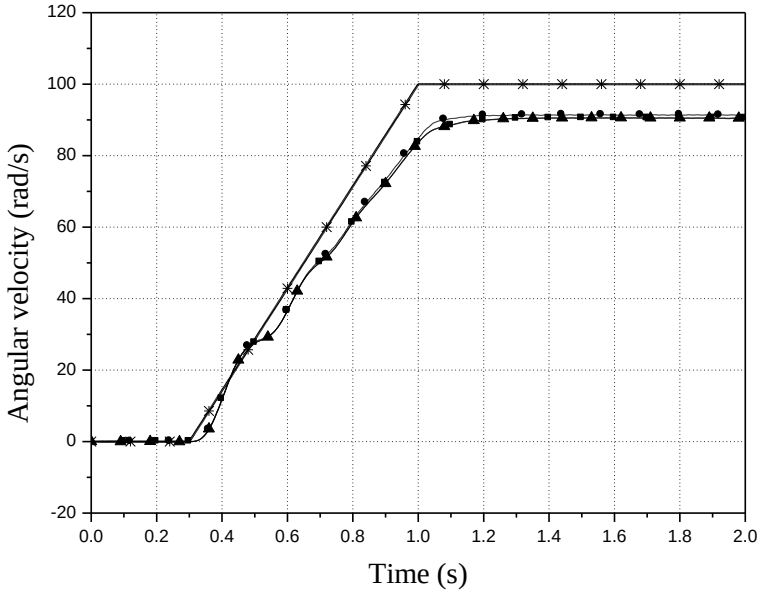

Figure 4 Angular velocity of the driving and driven pulleys
(—✳—Driving pulley,—●— C^1 belt (driven pulley), —▲— C^0/C^1 belt (driven pulley),
- -■- - chain (driven pulley))

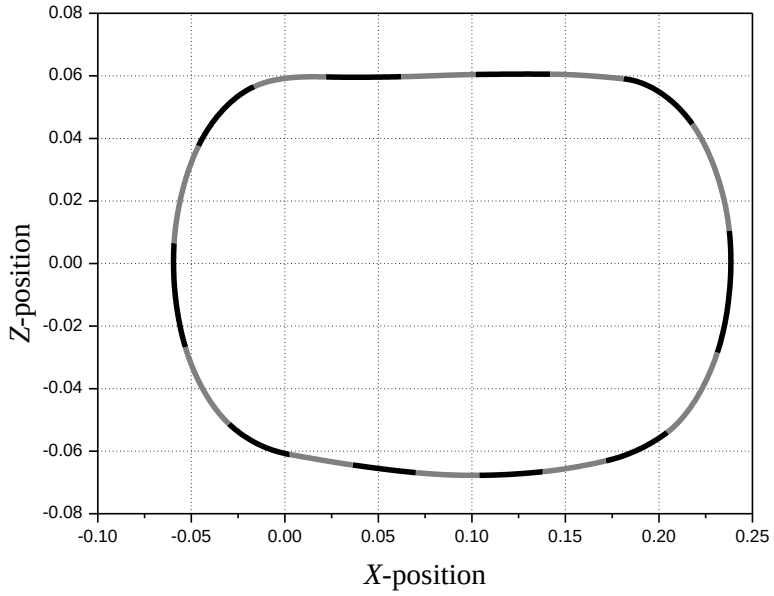

Figure 5 Centerline of the C^1 belt model at time 1s

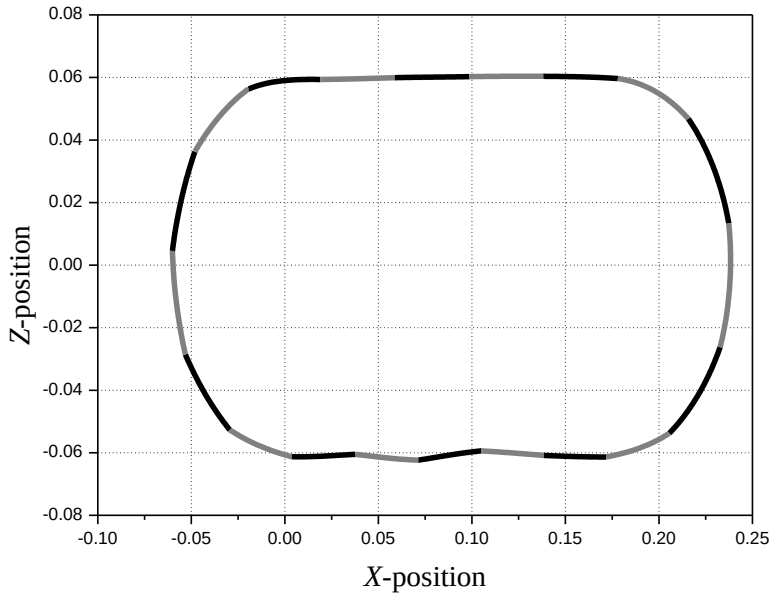

Figure 6 Centerline of the C^0/C^1 belt model at time 1s

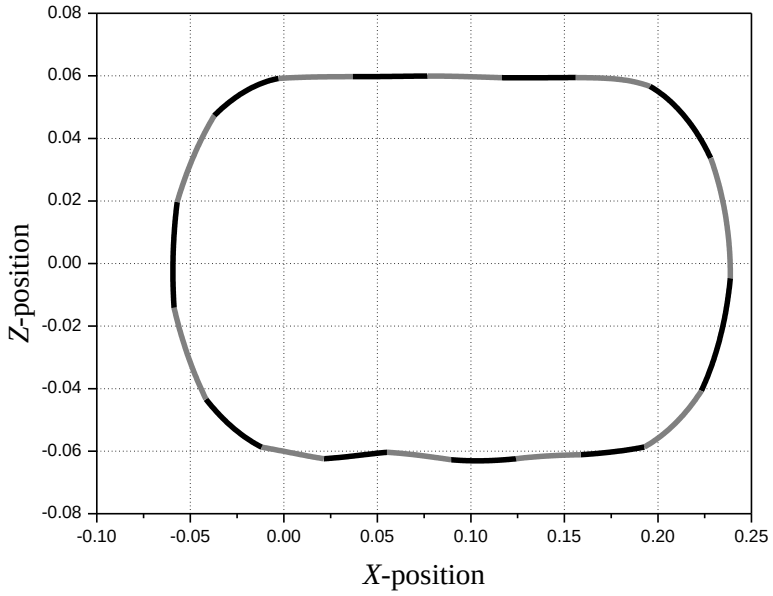

Figure 7 Centerline of the chain model at time 1s

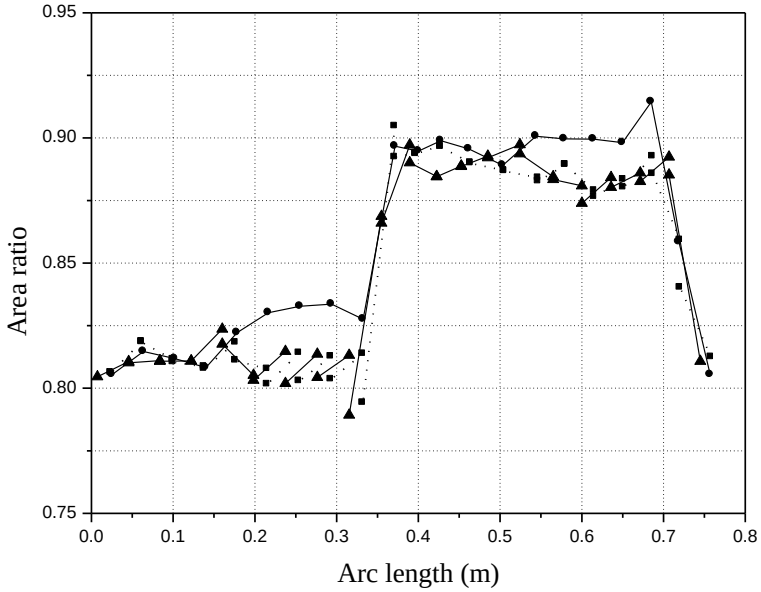

Figure 8 Area ratio along the belt centerline at time 1.9s
(—●— C^1 belt,—▲— C^0/C^1 belt, - ■ - chain)

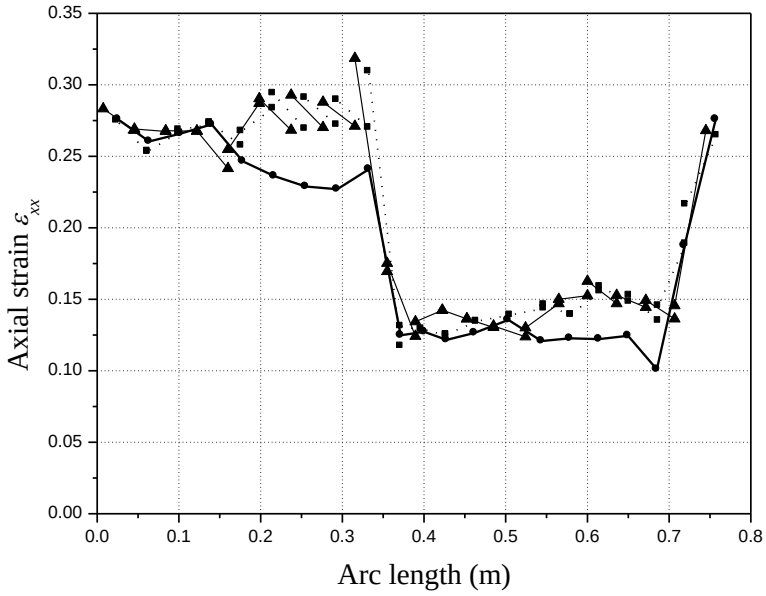

Figure 9 Axial strain ε_{xx} along the belt centerline at time 1.9s

(—●— C^1 belt,—▲— C^0/C^1 belt, - ■ - chain)

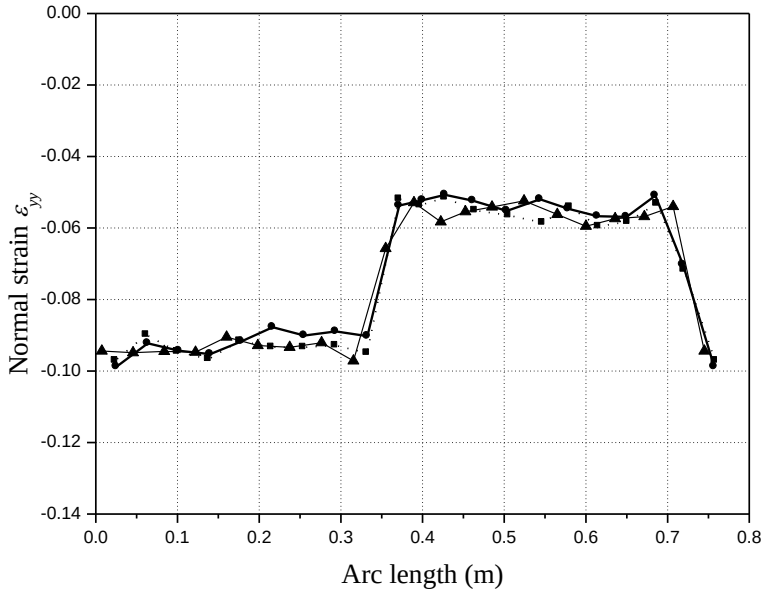

Figure 10 Normal strain ε_{yy} along the belt centerline at time 1.9s

(—●— C^1 belt,—▲— C^0/C^1 belt, - ■ - chain)

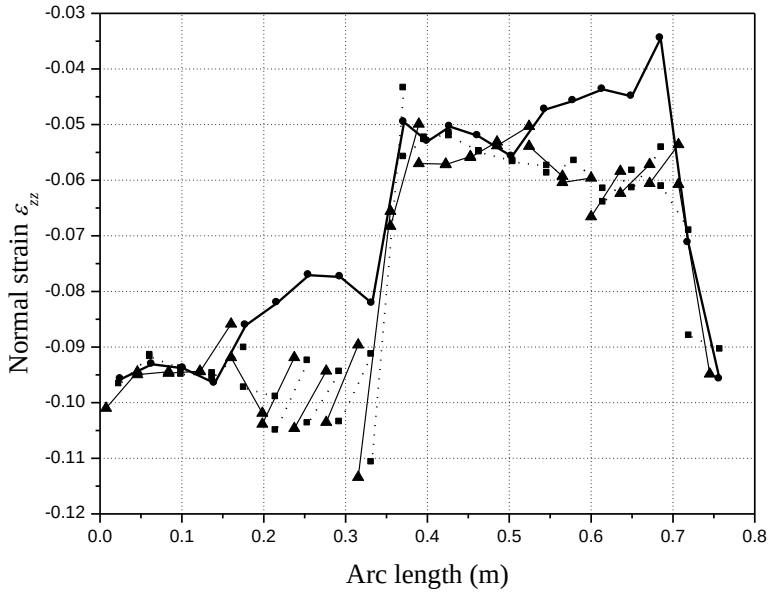

Figure 11 Normal strain ε_{zz} along the belt centerline at time 1.9s

(—●— C^1 belt,—▲— C^0/C^1 belt, - ■ - chain)

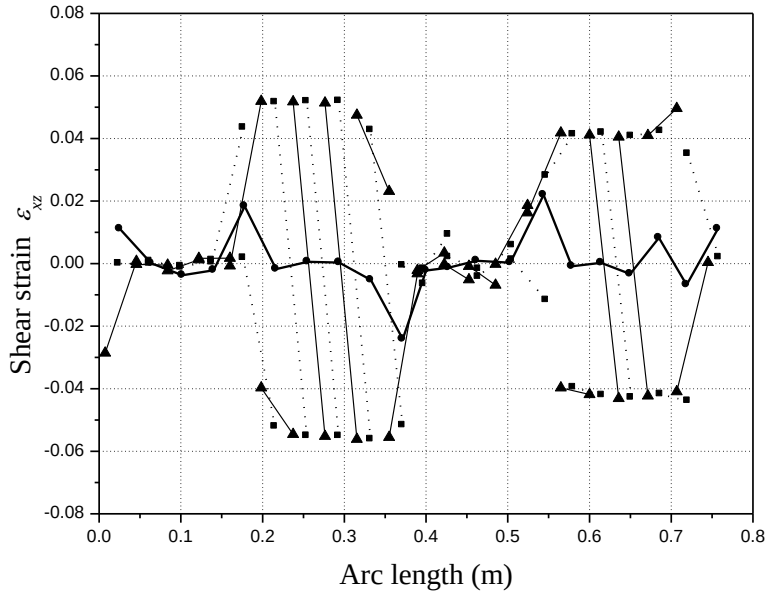

Figure 12 Shear strain ε_{xz} along the belt centerline at time 1.9s

(—●— C^1 belt,—▲— C^0/C^1 belt, - ■ - chain)